Int. J. Heat Mass Transfer. Vol. 34, No. 11, pp. 2739–2749, 1991
Printed in Great Britain

0017–9310/91 $3.00 + 0.00

Numerical prediction for laminar forced convection in parallel-plate channels with transverse fin arrays

CHIN-HSIANG CHENG and WEN-HSIUNG HUANG
Department of Mechanical Engineering, Tatung Institute of Technology, 40 Chungshan North Road Sec. 3, Taipei, Taiwan, R.O.C.

(*Received* 13 *April* 1990 *and in final form* 6 *December* 1990)

Abstract—A numerical study is performed on the laminar forced convection in parallel-plate channels with two series of transverse fins. Velocity and temperature distributions of the periodically fully-developed flow are carried out through a stream function–vorticity transformation with a finite difference scheme. Based on the obtained solutions of flow field, the effect of Reynolds number and other geometric parameters on the heat transfer coefficient and the friction factor can be further evaluated. Results show that the relative position of the fin arrays is an influential factor on the flow field, especially for the higher-fin cases. In general, the in-line arrangement behaves ineffectively due to the remarkable flow recirculation covering the wall surfaces.

1. INTRODUCTION

LAMINAR forced-convection flows in parallel-plate channels have been extensively studied in the last few decades. A comprehensive survey of the literature pertinent to the heat transfer behaviour and friction loss for the entrance and fully-developed regions has been provided by Shah and London [1]. However, since the overall heat transfer coefficients for a smooth channel are always insufficient for engineering application, the augmentation of heat transfer becomes particularly important.

In a real heat transfer device, fins or ribs are usually attached onto the wall surfaces in order to give additional area for heat transfer and to improve mixing of fluid. Forced convection flow in the channels with one single obstructive block [2, 3], multiple blocks [4], multiple transverse fins [5, 6], or fin arrays [7–12] has been investigated numerically and experimentally to study the separation and reattachment phenomena as well as their influence on heat transfer performance.

As two series of fins are mounted on the respective walls of a channel, the flow is expected to attain, after a short entrance length, a 'periodic' fully-developed character [9, 10]. For analysing this character, Rowley and Patankar [11] dealt with the numerical computation for a circular tube with an array of circumferential internal fins. Kelkar and Patankar [7] solved a similar problem in a parallel-plate channel with staggered fins. Based on their results, it is found that the staggered arrangement performs better in heat transfer than the in-line arrangement. Physically speaking, this is seemingly because the staggered fins can cause the flow to deflect and impinge upon the opposite walls, whereas the in-line fins make passing flow detach from the channel walls and hence, reduce the heat transfer performance on the wall surfaces.

According to the numerical data provided by ref. [7], Lazaridis [12] presented a correlation formula between Nusselt number and the physical parameters for practical application. Besides, Webb and Ramadhyani [8] found that conduction in the channel wall can play a highly beneficial role in enhancing heat transfer in a channel with staggered fins.

However, although the relative position of the two fin arrays, varying between staggered and in-line arrangements, is 'recognized' to be an influential factor to the flow, no direct information is available for evaluating such an influence yet. Hence, it is necessary to study the effect of the relative position in order to find an effective arrangement.

Meanwhile, it is important to note that due to the existence of fins, the heat transfer coefficient may be altered; however, along with the increase of heat transfer, there always comes an increase in pressure drop. Therefore, it needs a careful evaluation for the thermal and flow fields to assess the advantage of a proposed heat transfer augmentation technique.

Under these circumstances, this study performs the numerical prediction of heat transfer and flow pattern behaviours for the periodic fully-developed flow and treats the relative position of fin arrays as an important variable. Various physical arrangements are considered in order to investigate their influence on the thermal characteristic and friction loss.

The parallel-plate channel with fin arrays mounted on the respective walls is shown in Fig. 1. Since the geometry shown in this figure contains a series of identical modules, the velocity field repeats itself from module to module periodically after a short entrance region [9, 10]. It is thus possible to calculate

NOMENCLATURE

D_h	hydraulic diameter
d	pitch of fin array
e	fin height
f	friction factor, equation (15)
H	channel width
$\bar{h}$	average heat transfer coefficient
k	thermal conductivity of fluid
L	relative position of two fin arrays
Nu_x	local Nusselt number on wall, equation (26)
$\overline{Nu}$	average Nusselt number, equation (27)
P	dimensionless fluid pressure, equation (14)
Pr	Prandtl number
p	fluid pressure
$\bar{p}$	periodic variation part of pressure, equation (3)
$\bar{p}_o$	reference pressure
Q_b	dimensionless overall heat transfer on wall
Q_{bx}	dimensionless local heat flux on wall, equation (23)
Q_f	dimensionless overall heat transfer on fin surfaces
Q_{fy}	dimensionless local heat flux on fin surface, equation (24)
Q_t	dimensionless total heat transfer in a module, equation (25)
q_i	local heat flux on wall i, $i = 1$ or 2
q_t	total heat flux in a module
Re	Reynolds number, equation (11)
T	fluid temperature
T_m	bulk mean temperature of flow
U	dimensionless fluid velocity in the x-direction
u	fluid velocity in the x-direction
u_m	average axial velocity
V	dimensionless fluid velocity in the y-direction
v	fluid velocity in the y-direction
W	dimensionless fluid vorticity, equation (8)
w	fluid vorticity
X, Y	dimensionless coordinates
x, y	rectangular coordinate system.

Greek symbols

θ	dimensionless fluid temperature
ν	kinematic viscosity of fluid
τ	global pressure gradient
φ	stream function
ψ	dimensionless stream function
ψ_m	maximum value of dimensionless stream function in the recirculating eddy.

Subscripts

L	left surface of fin
o	smooth channel
R	right surface of fin
1	wall 1
2	wall 2.

the flow pattern and heat transfer behaviours in a unit module (such as A–B–C–D) without the need of computation for the entrance region.

The fins with fin height (e) are placed uniformly at a pitch (d) in each fin series. However, the relative position of fin arrays (L) may be altered during the computation to study the effect of L on the flow field. It is noted that $L = 0$ represents an exactly in-line arrangement, whereas $L = d/2$ denotes an exactly staggered arrangement for the fin arrays.

The channel walls are maintained with uniform but not equal surface temperatures. Based on the concepts of periodic fully-developed character advanced by Patankar *et al.* [10], the shapes of the temperature profiles at successive streamwise locations separated by one pitch will become approximately identical after a thermal entrance length, under such an asymmetrically isothermal boundary condition. The periodic behaviour of the temperature field enables the flow field and heat transfer analyses to be confined to a single module simultaneously.

The present study provides the numerical solutions for different Reynolds numbers (up to 500) and for various geometric parameters e/H and L/H, with

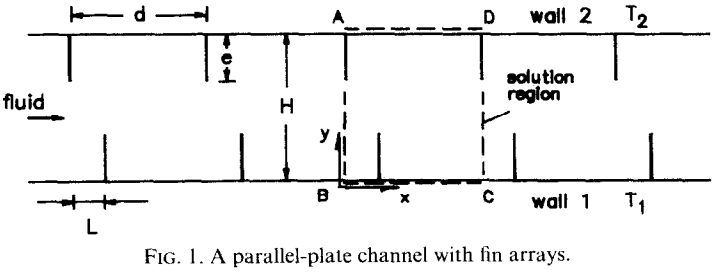

FIG. 1. A parallel-plate channel with fin arrays.

$d/H = 2$. The fin material is assumed to be perfectly conductive so that the temperatures on fin surfaces are equal to the related wall temperatures. It is noted that the assumption of steady laminar flow in this study is basically valid according to the evidence provided by ref. [9]. However, since the influence of the relative position on the vortex shedding has not yet been evaluated, a further experimental investigation for this is definitely needed.

2. ANALYSIS

The stream function–vorticity method is applied in the present work. Without the awkwardness in the pressure term treatment, this method inherently exhibits the merit in saving the computation time in calculation under the periodic conditions.

Since the basic computation procedures for the periodic fully-developed flows have been described in detail in refs. [7, 8, 10], the statement in the following section will be limited to the main features of the mathematical formulation and the treatment of boundary conditions.

2.1. *Flow field*

As explained in ref. [10], the velocity components u, v in a periodic fully-developed flow can be written with

$$u(x, y) = u(x+d, y) \tag{1}$$

$$v(x, y) = v(x+d, y). \tag{2}$$

The pressure is expressed by

$$p(x, y) = -\tau x + \tilde{p}(x, y) \tag{3}$$

where τ is a constant representing the global pressure gradient, and the quantity $\tilde{p}(x, y)$ is the periodic variation term with

$$\tilde{p}(x, y) = \tilde{p}(x+d, y). \tag{4}$$

Assuming that the flow is two-dimensional with constant properties and introducing equation (3) into the momentum equations, one obtains the continuity equation and momentum equations as

$$\frac{\partial u}{\partial x} + \frac{\partial v}{\partial y} = 0 \tag{5}$$

$$u\frac{\partial u}{\partial x} + v\frac{\partial u}{\partial y} = \frac{\tau}{\rho} - \frac{1}{\rho}\frac{\partial \tilde{p}}{\partial x} + \nu\left(\frac{\partial^2 u}{\partial x^2} + \frac{\partial^2 u}{\partial y^2}\right) \tag{6a}$$

$$u\frac{\partial v}{\partial x} + v\frac{\partial v}{\partial y} = -\frac{1}{\rho}\frac{\partial \tilde{p}}{\partial y} + \nu\left(\frac{\partial^2 v}{\partial x^2} + \frac{\partial^2 v}{\partial y^2}\right). \tag{6b}$$

The boundary conditions for the above equations are specified by the no-slip requirement on the channel walls and fin surfaces, and by the periodic behaviour of u, v and p at the upstream and downstream faces of the module. However, the boundary conditions do not involve the mass flow rate. As a matter of fact, the mass flow rate (or say, the Reynolds number) is related to the pressure gradient τ, which must be given beforehand. In the earlier studies [7, 8, 10, 11], the value of τ is iteratively adjusted in order to obtain the solution of velocity which leads to a desired flow rate or Reynolds number for a specific geometry. Such an iterative process, however, is a time-consuming step in the numerical procedure.

To reduce the computation effort, the stream function–vorticity method, in which there is no need to specify the value of the pressure gradient beforehand, is employed to examine the flow field, instead of the primitive variable method.

The continuity equation and the momentum equations, equations (5) and (6), can be transformed into a dimensionless stream function–vorticity formulation as

$$U = \frac{\partial \psi}{\partial Y}, \quad V = -\frac{\partial \psi}{\partial X} \tag{7}$$

$$W = \frac{\partial V}{\partial X} - \frac{\partial U}{\partial Y} \tag{8}$$

$$U\frac{\partial W}{\partial X} + V\frac{\partial W}{\partial Y} = \frac{2}{Re}\left(\frac{\partial^2 W}{\partial X^2} + \frac{\partial^2 W}{\partial Y^2}\right) \tag{9}$$

$$\frac{\partial^2 \psi}{\partial X^2} + \frac{\partial^2 \psi}{\partial Y^2} = -W \tag{10}$$

where $X = x/H$, $Y = y/H$, $U = u/u_m$, $V = v/u_m$, $\psi = \varphi/(u_m H)$ and $W = wH/u_m$. The Reynolds number is given by the hydraulic diameter of the channel D_h as

$$Re = u_m D_h/\nu. \tag{11}$$

In the above expressions, u_m refers to the average axial velocity.

It is noticed that the Reynolds number appears in the vorticity transport equation as an explicit parameter which can be specified directly. Hence, there is no need for an additional iterative process in the adjustment of the pressure gradient for a desired Reynolds number. The good agreement between the solutions in the present and the earlier studies will be shown later.

The periodic character of the dimensionless stream function and vorticity is also ensured with the periodic flow field, that is

$$W(X, Y) = W(X+d/H, Y) \tag{12}$$

$$\psi(X, Y) = \psi(X+d/H, Y) \tag{13}$$

where d/H is the dimensionless pitch length.

Once the velocity components U and V have been obtained, the pressure gradient can be further calculated through the momentum equation. Defining the dimensionless pressure and friction factor with

$$P = (\tilde{p} - \tilde{p}_0)/(\rho u_m^2) \tag{14}$$

and

$$f = \tau D_h/(\tfrac{1}{2}\rho u_m^2) \tag{15}$$

respectively, one may transform the momentum equation (6a) into

$$\frac{f}{4} - \frac{\partial P}{\partial X} = U\frac{\partial U}{\partial X} + V\frac{\partial U}{\partial Y} - \frac{2}{Re}\left(\frac{\partial^2 U}{\partial X^2} + \frac{\partial^2 U}{\partial Y^2}\right). \tag{16}$$

In equation (14), $\bar{p}_0$ is a reference pressure. By applying the periodicity conditions of P on the upstream and downstream faces, the friction factor can be calculated through the integration for equation (16) along the axial direction between two corresponding points on the respective faces, i.e.

$$f = 4(H/d)\int_0^{d/H}\left[U\frac{\partial U}{\partial X} + V\frac{\partial U}{\partial Y} - \frac{2}{Re}\left(\frac{\partial^2 U}{\partial X^2} + \frac{\partial^2 U}{\partial Y^2}\right)\right]\mathrm{d}X. \tag{17}$$

2.2. *Temperature field*

The dimensionless form of the energy equation is

$$U\frac{\partial \theta}{\partial X} + V\frac{\partial \theta}{\partial Y} = \frac{2}{Re\,Pr}\left(\frac{\partial^2 \theta}{\partial X^2} + \frac{\partial^2 \theta}{\partial Y^2}\right) \tag{18}$$

where $\theta = (T - T_2)/(T_1 - T_2)$, Prandtl number $Pr = 0.71$ for air, and T_1, T_2 represent the wall temperatures on walls 1 and 2, respectively. Under the asymmetrically isothermal heating conditions considered herein, the periodic character of the temperature field will be attained approximately in the fully-developed region with

$$\theta(X, Y) = \theta(X + d/H, Y). \tag{19}$$

The periodicity nature in stream function, vorticity and temperature, as well as the specified conditions on the solid surfaces are listed below:

on the bottom wall 1 and mounted fin surfaces

$$U = 0, \quad V = 0, \quad \psi = 0, \quad W = -\frac{\partial^2 \psi}{\partial N^2}, \quad \theta = 1; \tag{20}$$

on the top wall 2 and mounted fin surfaces

$$U = 0, \quad V = 0, \quad \psi = 1, \quad W = -\frac{\partial^2 \psi}{\partial N^2}, \quad \theta = 0; \tag{21}$$

at the upstream and downstream faces

$$\psi(0, Y) = \psi(d/H, Y) \tag{22a}$$

$$W(0, Y) = W(d/H, Y) \tag{22b}$$

$$\theta(0, Y) = \theta(d/H, Y) \tag{22c}$$

where N is the normal direction coordinate for the related solid surface.

2.3. *Numerical method*

By means of a finite difference scheme quite similar to that given in refs. [6, 13, 14], equations (7)–(10) and the energy equation (18) are solved to yield the velocity and temperature distributions in a single module. The power law scheme described in ref. [15] is employed for the treatment of convection terms in equations (9) and (18). A grid system of 101×51 grid points is adopted typically in this computation. However, a careful check for the grid-independence of the numerical solutions has been made to ensure the accuracy and validity of the numerical scheme. For this purpose, four grid systems, 51×41, 81×41, 101×51 and 101×66 are tested. It is found that for the case of $e/H = 0.5$, $L/H = 1$ with $Re = 500$, the relative error in the friction factor between the solutions of 101×51 and 101×66 is within 1%. However, the increase in computation time for the 101×66 system is considerable.

3. RESULTS AND DISCUSSION

3.1. *Results of flow field*

Figure 2 shows the significant effect of relative position of fin arrays on flow pattern for the case of $e/H = 0.3$ with $Re = 200$. It is noticed that in the staggered arrangement ($L/H = 1$), fluid is deflected by the fins to impinge upon the opposite channel walls. In the in-line arrangement ($L/H = 0$), the wall surfaces are covered by the recirculating eddies. The values of ψ_m indicated in this figure represent the ratios of the flow rates in different recirculating eddies to the overall passing flow rate.

The effect of the fin array's relative position on the flow pattern is shown in Fig. 3 for $e/H = 0.5$ and $Re = 200$. In this case with higher fins, a severe flow distortion is found as the value of L/H varies. However, the value of L/H should not be too close to zero, in order to avoid unstable vortex shedding near fin tips.

The influence of Reynolds number on flow field is shown in Fig. 4 for $e/H = 0.5$ and $L/H = 1$. As Reynolds number varies from 100 to 500, the strength of recirculating eddies is raised appreciably but the size of eddies is only slightly affected. Besides, since this very configuration was also considerd by Kelkar and Patankar [7], the flow pattern presented in Fig. 4 can be further compared with their results for confirmation. In consequence, a good agreement between the two sets of data has been found.

3.2. *Results of temperature field*

Figure 5 shows the effect of relative position of fin arrays on the temperature distribution for $e/H = 0.5$ with $Re = 200$. The temperature field clearly exhibits a great dependence on the value of L/H. Basically, higher local heat transfer can be expected in the areas near the fin tips or fluid-impingement points on the

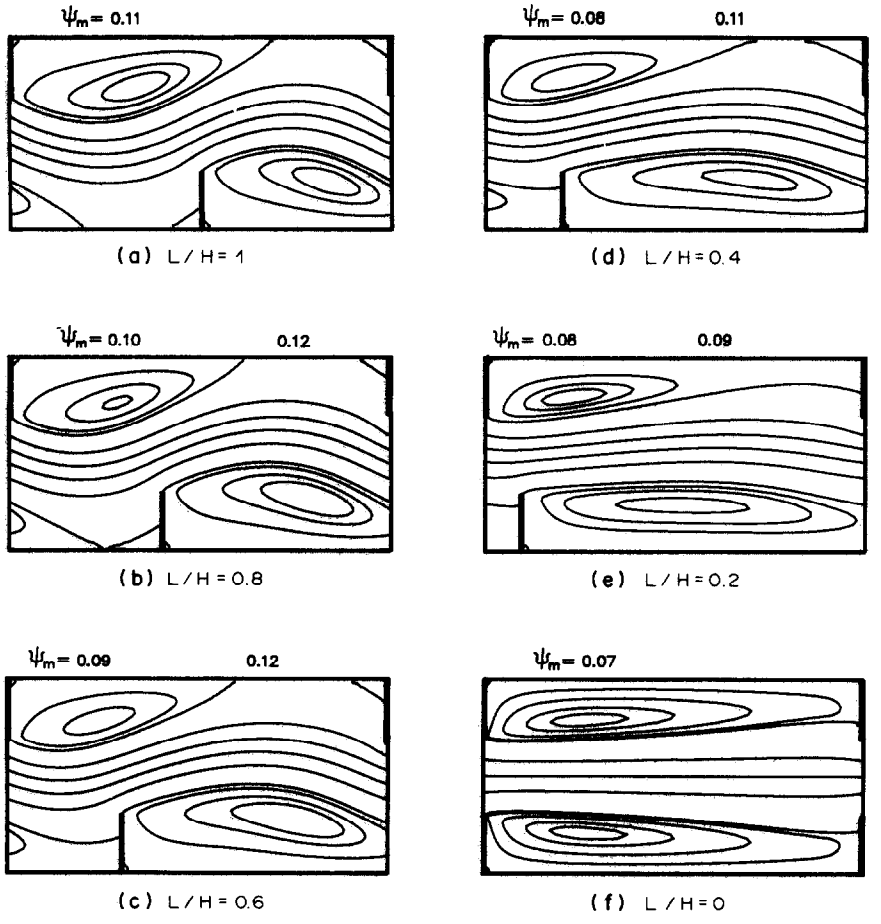

FIG. 2. Effect of relative position of fin arrays on flow pattern for $e/H = 0.3$ and $Re = 200$.

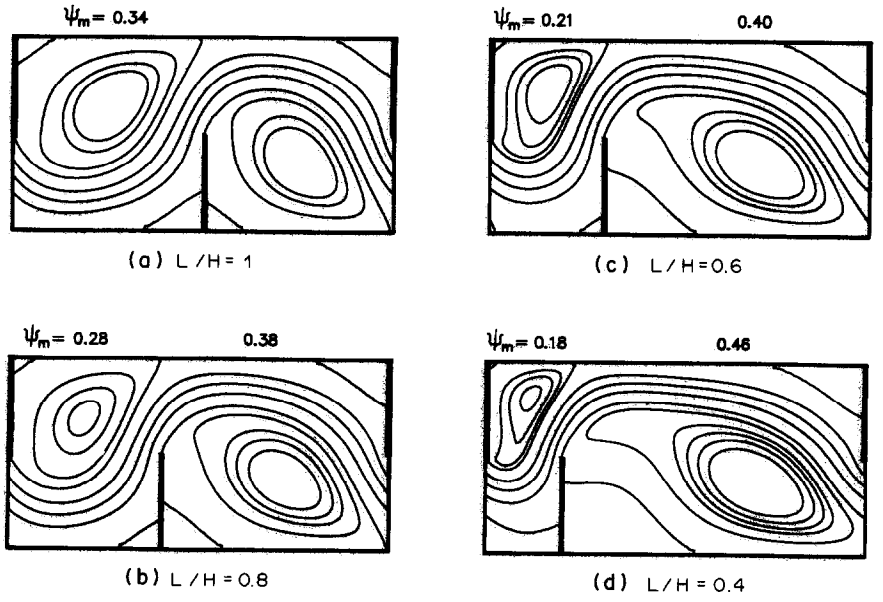

FIG. 3. Effect of relative position of fin arrays on flow pattern for $e/H = 0.5$ and $Re = 200$.

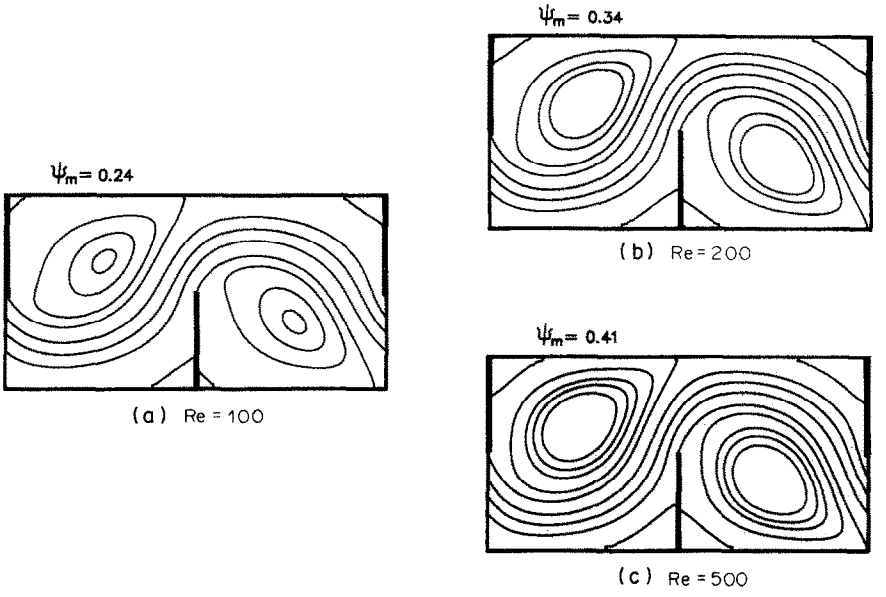

FIG. 4. Effect of Reynolds number on flow pattern for $e/H = 0.5$ and $L/H = 1$.

walls. However, the heat transfer reduction is also found at the rear of the fins due to the 'insulation effect' of the recirculating eddies.

The effect of fin height on the temperature field, for $L/H = 0.4$, is shown in Fig. 6. It is recognized that as the value of e/H diminishes, the solution approaches that of the smooth channel in which the fully-developed temperature profile is linear at any cross-section.

Figure 7 shows the influence of Reynolds number on the thermal field. For the case of $e/H = 0.5$ and $L/H = 1$, a stronger convection obviously takes place as the Reynolds number increases.

3.3. *Results of heat transfer and friction loss*

The solutions of temperature and velocity enable the heat transfer performance and the friction factor to be further evaluated. The dimensionless local heat flux on wall 1, Q_{bx}, is defined by

$$Q_{bx} = -\frac{H}{T_1 - T_2}\left.\frac{\partial T}{\partial y}\right|_{\text{wall 1}} = -\left.\frac{\partial \theta}{\partial Y}\right|_{\text{wall 1}}. \quad (23)$$

Meanwhile, the dimensionless local heat flux on the fin mounted on wall 1, Q_{fx}, is given by

$$Q_{fx} = \pm\frac{H}{T_1 - T_2}\left.\frac{\partial T}{\partial x}\right|_{\text{fin}} = \pm\left.\frac{\partial \theta}{\partial X}\right|_{\text{fin}} \quad (24)$$

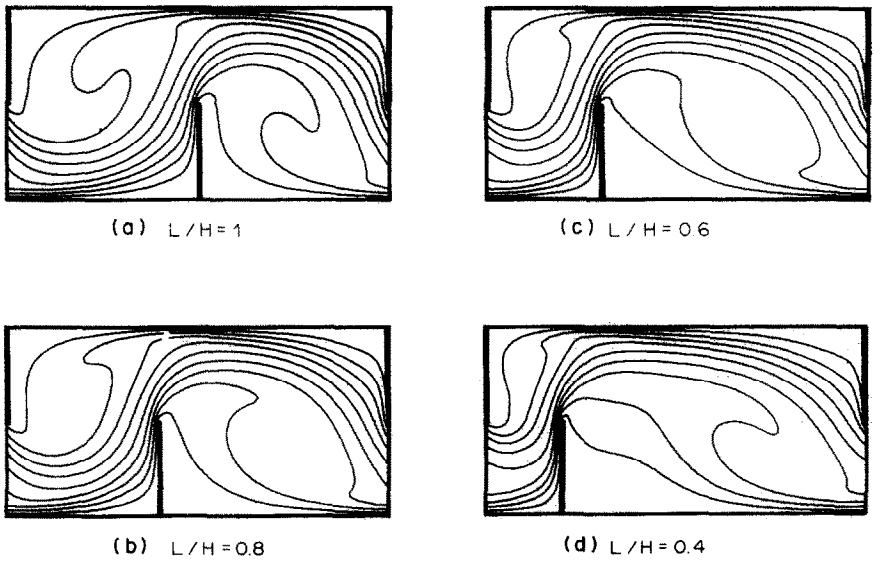

FIG. 5. Effect of relative position of fin arrays on temperature distribution for $e/H = 0.5$, $Pr = 0.71$ and $Re = 200$.

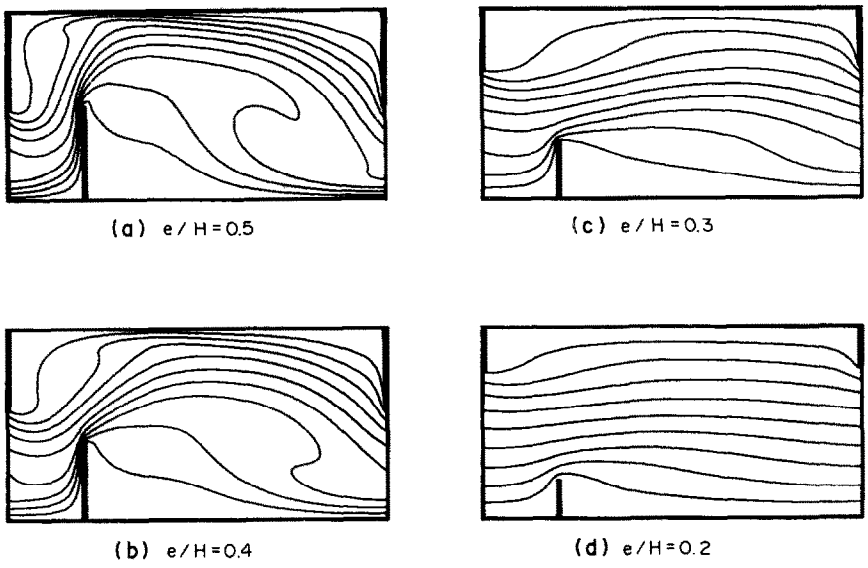

FIG. 6. Effect of fin height on temperature distribution for $L/H = 0.4$, $Pr = 0.71$ and $Re = 200$.

where the positive sign is selected for the left surface, and the negative sign for the right surface.

Integration of Q_{bx} along the wall surface from $X = 0$ to d/H yields the overall heat transfer on the wall Q_b. On the other hand, the overall heat transfer on the fin surfaces Q_f can also be calculated through the integration of Q_{fy}. Then the total heat transfer in a module can be calculated by

$$Q_t = Q_b + Q_f. \tag{25}$$

Assuming that $T_1 > T_2$, the total heat transfer from wall 1 and its mounted fin (Q_{t1}) should be equal to that from the fluid to wall 2 and the mounted fin (Q_{t2}), based on the energy balance for the module. However, in spite of the heat transfer from the fin surfaces, the overall heat transfer from wall 1 (Q_{b1}) can be different from that to wall 2 (Q_{b2}).

The local and average Nusselt number are given, respectively, as

$$Nu_x = q_i D_h/[k(T_i - T_m)], \quad i = 1 \text{ or } 2 \tag{26}$$

$$\overline{Nu} = \bar{h} D_h/k \tag{27}$$

where q_i is the local heat flux on wall i, T_m the bulk mean temperature defined by

$$T_m = \int_0^H |u| T \, dy \Big/ \int_0^H |u| \, dy$$

and $\bar{h} = q_t/[d(T_1 - T_m)]$ with q_t the total heat flux in a module.

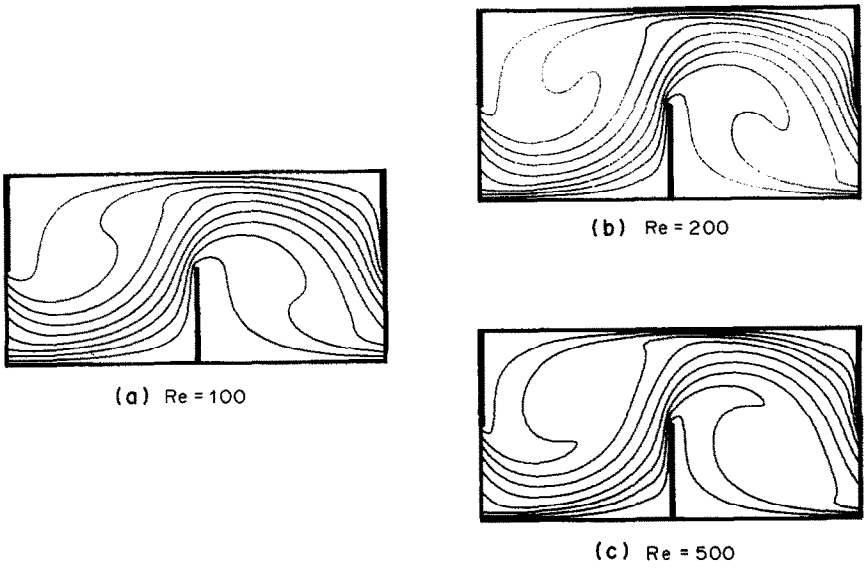

FIG. 7. Effect of Reynolds number on temperature distribution for $e/H = 0.5$, $L/H = 1$ and $Pr = 0.71$.

Based on the data provided by Shah and London [1], the Nusselt number, the total heat transfer and the value of $f\ Re$ for smooth channels within one module are

$$Nu_o = 4 \tag{28a}$$

$$Q_o = 2 \tag{28b}$$

$$(f\ Re)_o = 96 \tag{28c}$$

where the subscript 'o' refers to the smooth channel. The numerical results of the finned channel can then be compared with the above values to evaluate the effect of fins.

Figure 8 shows the predicted variation of friction factor $(f\ Re)/(f\ Re)_o$ as well as the total heat transfer Q_t/Q_o with fin height, for a staggered arrangement $(L/H = 1)$ with $Re = 200$. In general, both the friction factor and heat transfer increase with the value of e/H. The value of Q_t/Q_o reaches about 5 as e/H varies from 0 to 0.5, whereas the corresponding value of $(f\ Re)/(f\ Re)_o$ goes up to 60, much larger than that of heat transfer. The reason for the large pressure gradient is attributed to the serious distortion of the flow caused by the fins. Meanwhile, the numerical solutions of friction factor provided by Kelkar and Patankar [7] are also shown with the dashed line in this figure for comparison. A good agreement between the data of ref. [7] and the present study can be observed.

Figure 9 shows the effect of Reynolds number on friction factor and heat transfer. Unlike the smooth channel case, the results of the finned channel exhibit a strong dependence on Reynolds number. Both the friction factor and overall heat transfer increase with the value of Re. It is noted that the friction factor may increase with a factor in excess of 100, whereas only about a factor of 10 in Q_t/Q_o can be achieved. The comparison between the results in friction factor of Kelkar and Patankar [7] and of this study is also made in this figure. The maximum relative error of about 9.5% is found in the case of $Re = 500$. However, the error decreases rapidly as Reynolds number decreases.

The comparison in heat transfer could not be done

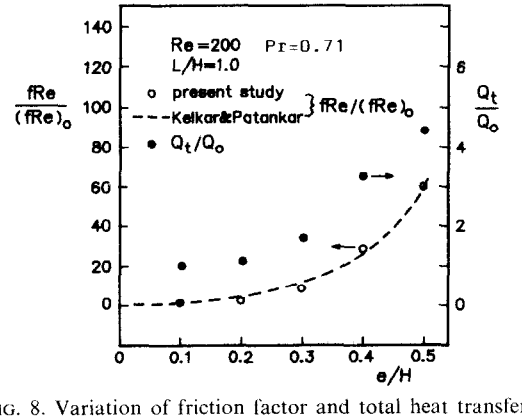

FIG. 8. Variation of friction factor and total heat transfer with fin height for $L/H = 1$, $Pr = 0.71$ and $Re = 200$, compared with ref. [7].

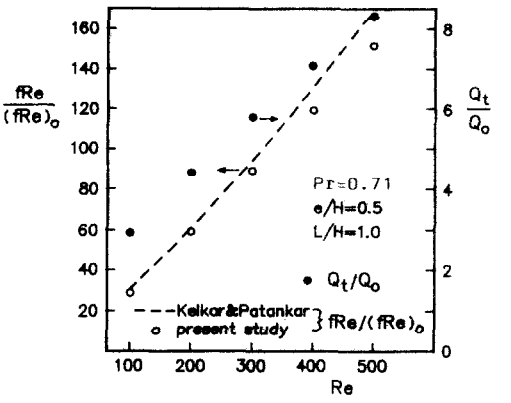

FIG. 9. Variation of friction factor and total heat transfer with Reynolds number for $e/H = 0.5$, $L/H = 1$ and $Pr = 0.71$, compared with ref. [7].

in Figs. 8 and 9 due to the lack of heat transfer data in earlier studies for the asymmetric heating condition. However, results of average Nusselt number of the present asymmetric heating case are listed in Table 1 together with some data of symmetric heating in refs. [7, 12] for a complete view.

Considering only the overall heat transfer on the wall surface (Q_b), the subtle effect of relative position of fin arrays can be further investigated. For $e/H = 0.3$ with $Re = 200$, Fig. 10 shows the variation of overall heat transfer on wall 1 with the value of L/H. The influence of Prandtl number is also displayed in this figure. It is clear that, for $Pr = 0.71$, the value of Q_b/Q_o is less than unity as $L/H = 0$, implying the decrease in heat transfer under this arrangement. But as $L/H = 1$, the flow distortion causes fluid impingement on the wall and makes Q_b/Q_o greater than unity.

For $Pr = 4$, it is seen that the heat transfer is obviously greater than that for $Pr = 0.71$. However, it is also clear that the staggered arrangement behaves more efficiently in heat transfer than the in-line one.

On the other hand, the effect of the fin height as well as the relative position of fin arrays on the friction factor for $Re = 200$ is shown in Fig. 11. The value of $(f\ Re)/(f\ Re)_o$ has a great dependence on both the values of L/H and e/H. In general, for any L/H value, the friction factor decreases monotonously with e/H. But for different fin heights, it displays different variation trends in friction factor as L/H varies from 0 to 1. However, for the higher-fin cases $(e/H > 0.3)$, the effect of L/H on friction factor becomes more significant. A similar feature can be observed for other Reynolds numbers.

Figure 12 shows the data of friction factor and total heat transfer for various Reynolds numbers as $e/H = 0.2$ and $L/H = 0.6$.

The distribution of local Nusselt number on the wall surfaces is displayed in Fig. 13. For the staggered case, $L/H = 1$ and $e/H = 0.5$, the Nusselt numbers increase with Reynolds number. The local maximum

Table 1. Average Nusselt number as a function of Re, Pr and heating condition for $L/H = 1$ and $e/H = 0.5$

	$\overline{Nu}/Nu_0$			
	$Pr = 0.71$		$Pr = 4.0$	
Reynolds number	Symmetric heating [7, 12]	Asymmetric heating (present)	Symmetric heating [7, 12]	Asymmetric heating (present)
100	2.25	2.901	3.9	5.934
200	3.3	4.390	6.8	11.140
300	4.4	5.758	9.4	15.082
400	5.3	7.062	11.7	18.144
500	6.233	8.295	13.441	20.508

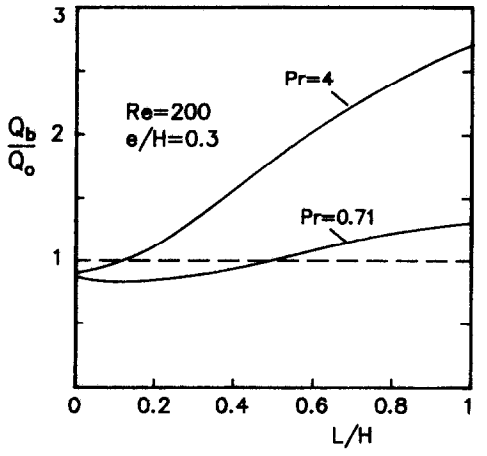

FIG. 10. Effect of relative position of fin arrays on the overall wall heat transfer for $e/H = 0.3$ and $Re = 200$.

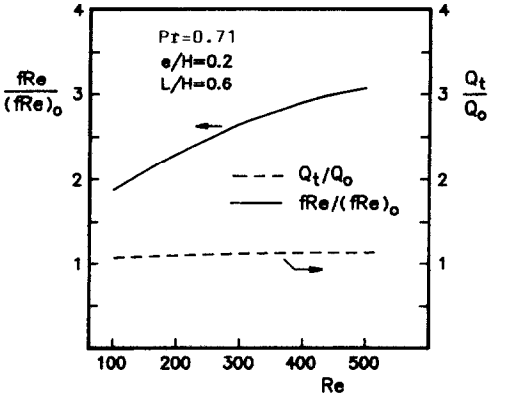

FIG. 12. Variation of friction factor and total heat transfer with Reynolds number for $e/H = 0.2$, $L/H = 0.6$ and $Pr = 0.71$.

in Nu_x/Nu_0 on the wall seemingly occurs at the point where the impingement of the flow is strongest. However, in the areas adjacent to the fin (whose position is indicated by the dashed line in this figure), a poor heat transfer due to the local stagnant flow is found.

Figure 14 shows the influence of the fin array's relative position on Nu_x/Nu_0 on the respective walls, for $e/H = 0.3$ with $Re = 200$. The dashed curves provided are associated with the top wall 2. For $L/H = 0$ (in-line arrangement), the distributions of heat transfer coefficient on wall 1 and wall 2 are identical. Therefore, only one curve for this case is given here.

Figure 15 shows the great influence of Reynolds number on local heat transfer on the fin surfaces, for the case of $L/H = 1.0$ and $e/H = 0.5$. It is observed that due to higher temperature and velocity gradients at the fin tip, the local heat transfer there is obviously larger than other points on both surfaces.

It is important to remention that for the special case of $e/H = 0$ (i.e. a smooth channel) the numerical solutions of velocity and temperature profiles approach exactly the Poiseuille velocity profile and the linear

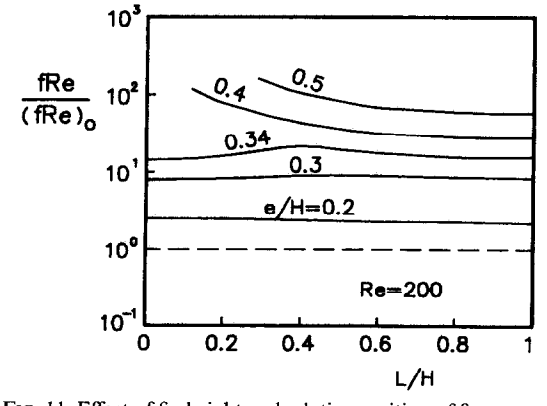

FIG. 11. Effect of fin height and relative position of fin arrays on friction factor for $Re = 200$.

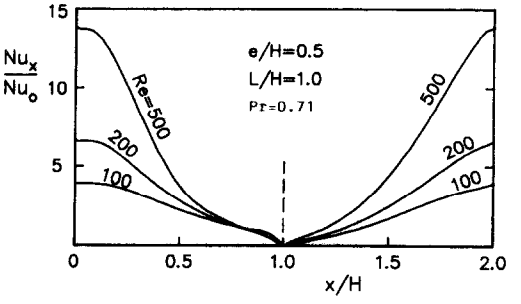

FIG. 13. Effect of Reynolds number on local Nusselt number on walls for $e/H = 0.5$, $L/H = 1$ and $Pr = 0.71$.

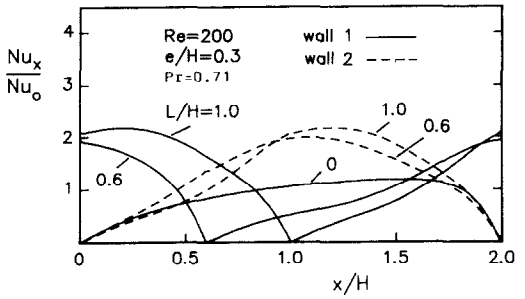

FIG. 14. Effect of relative position of fin arrays on local Nusselt number on walls for $e/H = 0.3$, $Pr = 0.71$ and $Re = 200$.

temperature distribution [1] of the fully-developed flow, respectively. Figure 16 shows the results of comparison between numerical and analytical solutions. This agreement can also ensure the accuracy of numerical prediction.

4. CONCLUSIONS

Numerical investigation on the heat transfer and flow pattern for the laminar forced convection in the parallel-plate channels with conductive fin arrays has been carried out. The effect of the physical parameters, $10 \leqslant Re \leqslant 500$, $0 \leqslant e/H \leqslant 0.5$, $0 \leqslant L/H \leqslant 1$ and $Pr = 0.71$ or 4 is evaluated by the stream function–vorticity method with the finite difference scheme.

Basically, when two series of perfectly conductive fins are mounted on the respective walls, the flow will attain a periodic fully-developed character after a short entrance length. In this region, both the heat transfer and friction factor of the flow are found to be dependent on the Reynolds number and the geometric arrangement.

The relative position of the fin arrays (L/H) is treated as another influential parameter to the flow. The flow pattern with the configuration varying from in-line to staggered arrangement is predicted. Results show that the friction factor exhibits greater dependence on the relative position of fin arrays for the higher-fin cases ($e/H > 0.3$).

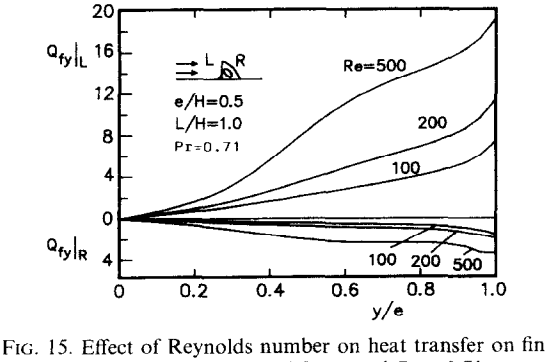

FIG. 15. Effect of Reynolds number on heat transfer on fin surfaces for $e/H = 0.5$, $L/H = 1$ and $Pr = 0.71$.

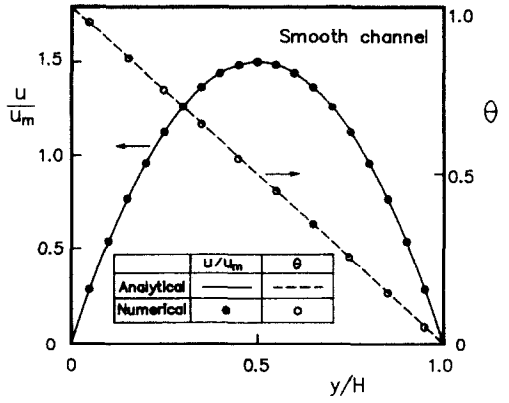

FIG. 16. Comparison between numerical and analytical solutions for the special case of a smooth channel.

For the improvement of overall wall heat transfer, the correct arrangement of fins is important. It is found that the in-line arrangement may cause the passing flow to detach from the wall, and hence result in the flow recirculation covering the wall surface. Consequently, a reduction in wall heat transfer may be caused. In respect of this, the staggered arrangement behaves more efficiently than the in-line one.

It is observed that both the total heat transfer and the friction loss may increase with Reynolds number and fin height. For the staggered (or nearly staggered) arrangement, the friction factor ratio, $(f\,Re)/(f\,Re)_o$, may increase by an order of 100, whereas only by about 10 in increasing of the total heat transfer ratio, Q_t/Q_o, can be achieved.

However, as the fin height diminishes, the solutions approach those of the fully-developed flow in a smooth channel and are independent of Reynolds number.

REFERENCES

1. R. K. Shah and A. L. London, Laminar flow forced convection in ducts. In *Advances in Heat Transfer* (Edited by T. F. Irvine and J. P. Hartnett), Supplement 1. Academic Press, New York (1978).
2. S. Bunditkul and W. J. Yang, Laminar transport phenomena in parallel channels with a short flow construction, *J. Heat Transfer* **101**, 217–221 (1979).
3. C. D. Tropea and R. Gackstatter, The flow over two-dimensional surface-mounted obstacles at low Reynolds numbers, *J. Fluids Engng* **107**, 489–494 (1985).
4. J. Davalath and Y. Bayazitoglu, Forced convection cooling across rectangular blocks, *J. Heat Transfer* **109**, 321–328 (1987).
5. F. Durst, M. Founti and S. Obi, Experimental and computational investigation of the two-dimensional channel flow over two fences in tandem, *J. Fluids Engng* **110**, 48–54 (1988).
6. C. H. Cheng and W. H. Huang, Laminar forced convection flows in horizontal channels with transverse fins placed in entrance regions, *Numer. Heat Transfer*, Part A **16**, 77–100 (1989).
7. K. M. Kelkar and S. V. Patankar, Numerical prediction of flow and heat transfer in a parallel plate channel with staggered fins, *J. Heat Transfer* **109**, 25–30 (1987).

8. B. W. Webb and S. Ramadhyani, Conjugate heat transfer in a channel with staggered ribs, *Int. J. Heat Mass Transfer* **28**, 1679–1687 (1985).
9. C. Berner, F. Durst and D. M. McEligot, Flow around baffles, *J. Heat Transfer* **106**, 743–749 (1984).
10. S. V. Patankar, C. H. Liu and E. M. Sparrow, Fully developed flow and heat transfer in ducts having streamwise periodic variation of cross-sectional area, *J. Heat Transfer* **99**, 180–186 (1977).
11. G. J. Rowley and S. V. Patankar, Analysis of laminar flow and heat transfer in tubes with internal circumferential fins, *Int. J. Heat Mass Transfer* **27**, 553–560 (1984).
12. A. Lazaridis, Heat transfer correlation for flow in a parallel-plate channel with staggered fins, *J. Heat Transfer* **110**, 801–802 (1988).
13. A. Bejan, *Convection Heat Transfer*, Chap. 12. Wiley, New York (1984).
14. P. J. Roache, *Computational Fluid Dynamics*, Chap. 3. Hermosa, Albuquerque, New Mexico (1972).
15. S. V. Patankar, *Numerical Heat Transfer and Fluid Flow*, Chap. 4. Hemisphere, Washington, DC (1980).

PREDICTION NUMERIQUE POUR LA CONVECTION FORCEE LAMINAIRE DANS DES CANAUX A PLAQUES PARALLELES AVEC DES ARRANGEMENTS DE PICOTS

Résumé—Une étude numérique est conduite sur la convection laminaire forcée dans un canal à plaques parallèles avec deux séries de picots transverses. Des distributions de vitesse et de température de l'écoulement établi périodique sont obtenues avec une transformation fonction de courant–vorticité avec un schéma de différences finies. A partir des solutions obtenues, on évalue l'effet de nombre de Reynolds et d'autres paramètres géométriques sur le coefficient de transfert thermique et le coefficient de frottement. Les résultats montrent que la position relative des picots est un facteur influant sur le champ de vitesse. En général, l'arrangement en ligne est moins afficace à cause de la recirculation de l'écoulement qui couvre les parois.

NUMERISCHE BERECHNUNG DER LAMINAREN ERZWUNGENEN KONVEKTION IN EINEM STRÖMUNGSKANAL AUS PARALLELEN PLATTEN MIT QUERVERLAUFENDER BERIPPUNG

Zusammenfassung—Die laminare erzwungene Konvektion in einem Kanal aus parallelen Platten mit zwei Reihen querverlaufender Rippen wird numerisch untersucht. Unter Verwendung eines Finite-Differenzen-Verfahrens und einer Transformation für Stromfunktion und Wirbelintensität ergeben sich die Verteilungen für Geschwindigkeit und Temperatur in der periodisch vollständig entwickelten Strömung. Aufgrund des berechneten Strömungsfeldes kann der Einfluß der Reynolds-Zahl und anderer geometrischer Parameter auf die Koeffizienten für Wärme- und Impulstransport bestimmt werden. Es zeigt sich, daß die relative Position der Rippenanordnungen einen starken Einfluß auf das Strömungsfeld ausübt—insbesondere in Fällen mit hohen Rippen. Ganz allgemein ist eine fluchtende Anordnung aufgrund der spürbaren Rezirkulationsströmung an der Wandoberfläche wenig wirksam.

ЧИСЛЕННОЕ ИССЛЕДОВАНИЕ ЛАМИНАРНОЙ ВЫНУЖДЕННОЙ КОНВЕКЦИИ В ПЛОСКОПАРАЛЛЕЛЬНЫХ КАНАЛАХ С ПОПЕРЕЧНЫМИ РЯДАМИ РЕБЕР

Аннотация—Численно исследуется ламинарная вынужденная конвекция в плоскопараллельном канале с двумя рядами поперечных ребер. Распредения скоростей и температур периодического полностью развитого течения определены с помощью преобразования "функция тока—завихренность" конечно-разностным методом. На основе полученных решений для поля течения может оцениваться влияние числа Рейнольдса и других геометрических параметров на коэффициенты теплопереноса и трения. Результаты показывают, что относительное расположение рядов ребер оказывает влияние на поле течения, особенно в случае ребер большой высоты. Коридорное расположение ребер является неэффективным в силу значительной рециркуляции течения у поверхностей стенок.